Sensors and Actuators B 233 (2016) 100–106

Contents lists available at ScienceDirect

Sensors and Actuators B: Chemical

journal homepage: www.elsevier.com/locate/snb

Electrochemical cholesterol sensor based on cholesterol oxidase and MoS_2-AuNPs modified glassy carbon electrode

Xiaoyun Lin[a,*], Yongnian Ni[a,b,*], Serge Kokot[c]

[a] College of Chemistry, Nanchang University, Nanchang 330031, China
[b] State Key Laboratory of Food Science and Technology, Nanchang University, Nanchang 330047, China
[c] School of Chemistry, Physics and Mechanical Engineering, Queensland University of Technology, Brisbane 4001, Australia

ARTICLE INFO

Article history:
Received 28 December 2015
Received in revised form 30 March 2016
Accepted 4 April 2016
Available online 6 April 2016

Keywords:
Biosensor
Molybdenum disulfide
Gold nanoparticle
Cholesterol oxidase

ABSTRACT

A novel modified electrode has been successfully constructed with the use of a nano-composite mixture consisting of molybdenum disulfide (MoS_2) and gold nanoparticles (AuNPs). Its application as a cholesterol biosensor was investigated. The morphology of the prepared MoS_2-AuNPs nanoparticles were characterized by scanning electron microscopy (SEM), transmission electron microscopy (TEM), atomic force microscope (AFM), X-ray diffraction (XRD) and energy dispersive X-ray spectroscopy (EDS). The physicochemical properties of the modified electrode at each stage of the construction were characterized by electrochemical impedance spectroscopy (EIS) and cyclic voltammetry (CV). Quantitative analysis of cholesterol was carried out with the use of the amperometric *i–t* method, and the calibration plot for cholesterol was linear in the range of 0.5–48 μM with a limit of detection (LOD) of 0.26 ± 0.015 μM. The apparent Michaelis-Menten constant (K_M^{app}) and sensitivity were estimated to be 0.325 mM and 4460 μA mM^{-1} cm^{-2}, respectively. This novel sensor produced satisfactory reproducibility and stability, and was used successfully for the quantitative analysis of cholesterol in egg yolk and pork liver samples.

1. Introduction

Cholesterol is an essential lipid produced by liver, and is crucial for normal body functioning. However, an excessive amount of cholesterol in the blood can significantly raise the risk of arterial disease [1]. The majority of coronary heart diseases, hypertension, atherosclerosis and dysfunction of the lipid metabolism have their origin in high levels of cholesterol in the blood serum, usually caused by an intake of food with high level cholesterol [2,3]. Consequently, accurate and fast determination of cholesterol concentrations is important for clinical diagnosis, and different methods have been used for this purpose, e.g. colorimetric [4,5], fluorometric [6–8], high-performance liquid chromatography (HPLC) [9], HPLC with electrochemical detection [10], gas-liquid chromatography [11], and gas chromatography-mass spectrometry (GC–MS) [12]. However, these methods require sample pre-treatments or component separation, and generally they consume reagents and time. For these reasons, it would be quite useful to develop some alternative methods, with low-cost, efficient and easy pre-treatment, for the analysis of cholesterol in food and clinical samples.

In recent years, enzymatic electrochemical biosensors have been developed considerably because they have some advantages, such as fast response, high sensitivity, and intrinsic selectivity. Thus, many types of biosensors specific for cholesterol oxidase (Chox) have been reported [13–22].

In fabrication of a cholesterol biosensor, Chox is most commonly used as the biosensing analyte. Chox catalyzes the oxidation of cholesterol to H_2O_2 and cholest-4-en-3-one, i.e. the enzymatic reaction with the use of Chox (as a receptor) is:

$$\text{Cholesterol} + O_2 \xrightarrow{Chox} \text{Cholest-4-en-3-one} + H_2O_2$$

The electro-oxidation current associated with the production of hydrogen peroxide can be detected at a suitable potential.

Recently, some research has been focused on unusual morphologies of molybdenum compound [23–25]. Nanotubes and bucky ball-like molecules composed of MoS_2 exhibit unusual surface and electronic properties [26,27], and are widely used as an important material in photo-electrochemistry, e.g. photo-catalytic hydrogen production and microelectronic applications [28–30].

MoS_2 and other transition metal dichalcogenides can form bulk crystals composed of two-dimensional, vertically stacked layers. Such structures are similar to that of graphene and have many

* Corresponding authors at: College of Chemistry, Nanchang University, Nanchang 330031, China.
E-mail addresses: linxiaoyun@ncu.edu.cn (X. Lin), ynni@ncu.edu.cn (Y. Ni).

http://dx.doi.org/10.1016/j.snb.2016.04.019
0925-4005/

different electronic and optical properties [31]. Sulfur on the surface of MoS_2 layer can interact with noble metals, such as gold nano-particles (AuNPs). The bond between MoS_2 and the gold nano-structures was found to act as a highly coupled gate capacitor with a reduced carrier-transport thermal-barrier and an increased thermal conductivity [32,33].

When AuNPs and MoS_2 were combined, their total surface area increased considerably and thus, more Chox molecules could be bound on the surfaces. Consequently, this resulted in the production of the largest catalytic current for cholesterol detection.

The aims of this investigation were: 1. to produce stable mixed films of Chox and MoS_2-AuNPs composite nano-material obtained with the use of a layer-by-layer construction method; 2. to research and develop a quantitative electroanalytical method for the analysis of cholesterol at the Nafion/Chox/MoS_2-AuNPs/GCE with the use of the amperometric *i–t* technique.

2. Experimental

2.1. Reagents

Hydrogen tetrachloroaurate tetrahydrate ($HAuCl_4{\cdot}4H_2O$), Nafion (perfluorinated ion-exchange resin, 5 wt.% solution – a mixture of lower aliphatic alcohols and water), cholesterol oxidase (Chox, enzyme commission number 1.1.3.6, from streptomyces species – lyophilized powder ≥20 units/mg protein), and cholesterol (water soluble) were purchased from Sigma-Aldrich Co., Shanghai. $NaMoO_4{\cdot}H_2O$ and L-cysteine were obtained from Shanghai Chemical Reagent Co., China. All other chemicals (Analytical Grade reagents) were obtained from Beijing Chemical Reagent Co., China and used without further purification. Phosphate buffer solution (PBS, 0.05 M, pH 7.0) was used as the supporting electrolyte, and was prepared from KH_2PO_4 and K_2HPO_4; the buffer (pH 7.0) was monitored with an Orion SA720 meter (US). Double-distilled water was used throughout the experiments.

2.2. Instrumentation

Electrochemical experiments were performed with the use of a CHI660A electrochemical workstation (Chenhua Apparatus Co., Shanghai) conjunction with a three-electrode system: the working electrode – a modified GCE (3 mm diameter), the counter electrode – a platinum wire, and the reference electrode – a saturated calomel electrode (SCE). Electrode potentials were reported with respect to the SCE. A cell stand (Model BAS C1A) was used for voltammetric scanning and to stir the solution during the preconcentration step.

Transmission electron microscopy (TEM) and energy dispersive X-ray spectroscopy (EDS), for measuring the structure and morphology of the resulting compounds, were carried out with the use of a JEM-2010 (JEOL Co., Japan), and the associated point and linear resolution were found to be 0.23 nm and 0.14 nm, respectively. The accelerating voltage was set at 200 kV. The sample was placed on a carbon-coated copper grid by depositing a drop of the test solution on the grid. It was dried in air at room temperature. Scanning electron microscopy (SEM) images were obtained using Quanta200F instrument (FEI Ltd., Tokyo, Japan). The samples were electro-deposited or dropped onto the detachable GCE. The power level was 20 kV.

The surface topography of MoS_2 was observed by atomic force microscope (AFM) test on Multimode Nanoscope IIIa Controllor (Veeco Instruments Ins., US). X-ray diffraction data were recorded with the use of a Bede D1 System (Bede Scientific Instruments, Durham, UK) using Cu Kα radiation (λ = 1.5406) and a Bragg angle range of 10°–70°.

2.3. Preparation of MoS_2

MoS_2 was synthesized with the use of a hydrothermal method involving sodium molybdate and cysteine. Thus, 0.25 g $Na_2MoO_4{\cdot}2H_2O$ was dissolved in water (25 mL). After an ultrasonication of 5 min, the solution was adjusted to pH 6.5 with 0.1 mol L^{-1} HCl. Then, 0.5 g of L-cysteine and 50 mL water were added to the solution followed by ultra-sonication for 10 min. The mixture was then transferred into a 100 mL Teflon-lined stainless steel autoclave and reacted at 200 °C for 36 h. After the solution was allowed to cool, the dark precipitate for each composite sample was collected by centrifugation, washed with double-distilled water and ethanol, and dried in a vacuum oven at 80 °C for 24 h.

2.4. Preparation of Nafion/Chox/MoS_2-AuNPs/GCE

Glassy carbon electrodes (GCE, 3 mm diameter) were polished with emery paper and alumina slurry; they were then successively rinsed with dilute nitric acid, ethanol, and distilled water in an ultrasonic bath. Thereafter, the electrodes were immersed in 0.25 mol L^{-1} H_2SO_4 and the potential at the electrodes was cycled in the range of −1.0 and 1.0 V until a steady potential was reached.

MoS_2 (1.0 mg) was added to the 1.0 mL 0.5% Nafion solution, which was then ultra-sonicated for 2 h so as to produce a homogenous mixture of MoS_2-Nafion; then, a suspension mixture (15 μL) was spread drop-wise over the surface of the above prepared GCE. The solvent was evaporated to dryness in air, and then the surface of the MoS_2/GCE was rinsed with double-distilled water. The electrode was then dried in air at room-temperature (25 °C).

The MoS_2/GCE was immersed in 1.0×10^{-3} mol L^{-1} $HAuCl_4$ solution containing 0.01 mol L^{-1} Na_2SO_4 and 0.01 mol L^{-1} H_2SO_4. The solution was electrolysed at −0.2 V (vs. SCE) for 30 s and the gold nanoparticles were then electrodeposited at the electrode. After a 30 s deposition, the particle size and the distribution appeared to be much more uniform and homogeneous [34]. Finally, the obtained electrode, MoS_2-AuNPs/GCE, was removed out and rinsed with double-distilled water.

A fresh Chox (1.0 mg mL^{-1}) solution was prepared in a PBS (pH 7.0), and 10 μL of this solution was dropped onto the MoS_2-AuNPs/GCE so as to fabricate a Chox/MoS_2-AuNPs/GCE electrode; then, 3.0 μL 0.05% Nafion was pipetted onto this modified electrode to form a protective layer [27]. The construction of the modified electrode was shown in Scheme 1. All the prepared modified electrodes were stored in a refrigerator at 4 °C.

2.5. Treatment of the egg yolk and pork liver samples

An egg yolk sample (0.20 g) was weighed and transferred to a 25 mL colorimetric tube equipped with a screw cap. Then, 0.5 mL 50% potassium hydroxide and 4.5 mL ethanol were added to the tube, which was then immersed in a water bath at 80 °C for 20 min; this tube was shaken vigorously every 5 min (total four times) to ensure good mixing. Subsequently, the tube was removed from the bath, and allowed to cool. Petroleum ether (10 mL) was then added, and the mixture was shaken for 1 min. After standing for 5 min, a 1.0 mL aliquot of the supernatant was transferred quantitatively into another 25 mL colorimetric tube, and the sample was evaporated almost to dryness at 65 °C. This sample was then dissolved in 4.0 mL glacial acetic acid for later electrochemical analysis (see Section 3.6).

Pork liver (well crumbed, 0.50 g) was weighed and transferred into a 25 mL colorimetric tube, and 0.5 mL 50% sodium hydroxide and 4.0 mL ethanol were added. As described above for the egg sample, the tube with the sample was placed into the water bath at 65 °C for 60 min and shaken vigorously every 15 min to mix the sample well. The tube was then removed, cooled, and 3 mL 15% sodium

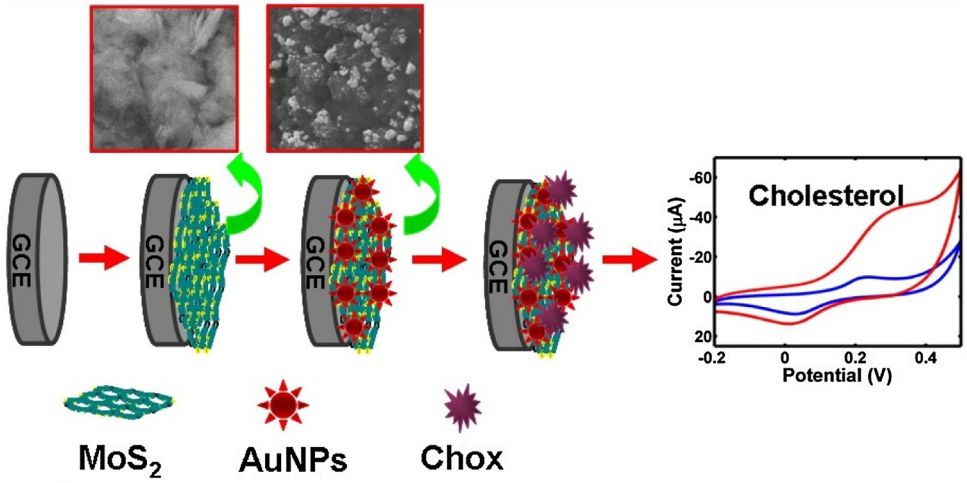

Scheme 1. A schematic representation of the fabrication of the Chox/MoS_2-AuNPs/GCE, and a possible reaction mechanism of cholesterol at the modified GCE.

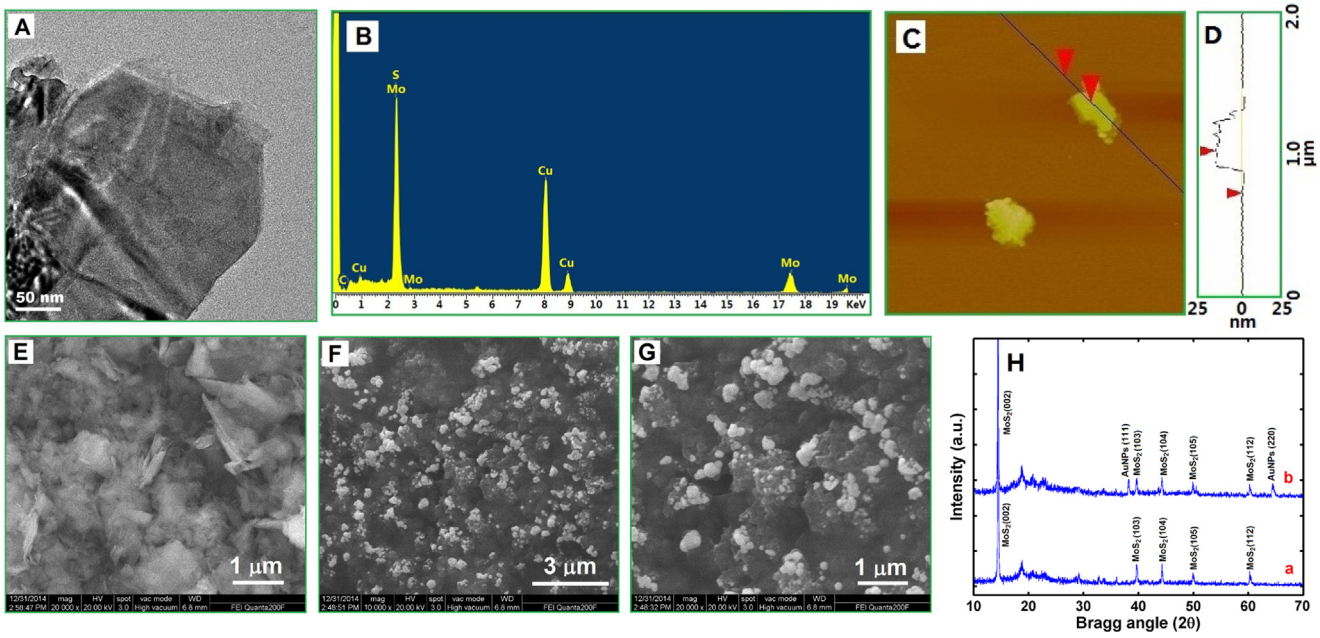

Fig. 1. (**A**) TEM image of MoS_2. (**B**) EDS of MoS_2. (**C**) AFM image of MoS_2. (**D**) The height chart of multilayered MoS_2. (**E**) SEM images of MoS_2/GCE. (**F** and **G**) SEM image of MoS_2-AuNPs/GCE. (**H**) XRD patterns of (**a**) MoS_2/GCE and (**b**) MoS_2-AuNPs/GCE.

chloride solution as well as 10 mL petroleum ether were added. The mixture was shaken for 2 min, and then allowed to stand for 5 min. At this point, a 2.0 mL aliquot of the supernatant was transferred into a 25 mL colorimetric tube and evaporated by a water bath (65 °C). The extract was dissolved in 4.0 mL glacial acetic acid for further study (see Section 3.6).

3. Results and discussion

3.1. Characterization of the MoS_2 –AuNPs/GCE

Fig. 1A was the TEM image of the prepared MoS_2 nanoparticles. It was observed that different layers were folded and tangled forming a multilayered morphology. EDS analysis was performed to characterize the chemical composition of MoS_2 (Fig. 1B) and confirmed the existence of the element Mo, S and Cu.

AFM characterization further confirmed that these as-prepared MoS_2 nanoparticles were multilayered (Fig. 1C). According to the literature [27], the height of monolayer MoS_2 was about 2–3 nm. From Fig. 1D, the height of these nanoparticles were approximately 16 nm (with 5–8 layers). This results were in agreement with TEM analysis.

The morphology of the MoS_2/GCE (Fig. 1E) and MoS_2-AuNPs/GCE (Fig. 1F and G) was investigated by SEM, and it could be observed that a very uneven, crumpled, and layered structure of the MoS_2 film seemed to form on the surface of the GCE (Fig. 1E). When AuNPs was electro-deposited on the surface of the MoS_2/GCE, it was obvious that the layered MoS_2 became a little aggregate and roughly cylindrical nano-particles were well distributed on the electrode's surface (Fig. 1F and G). The average diameter of these nano-particles was approximately 100 nm.

Fig. 1H showed the XRD pattern of the MoS_2 and MoS_2-AuNPs composites. It can be seen that diffraction of the substrate (GCE) shows a typical broad and weak reflection located in the range of 16–38°. The XRD pattern of the MoS_2 (curve a, Fig. 1H) has peaks at approximately 14°, 39°, 44°, 50° and 60°, which can be assigned to MoS_2 (002), (103), (104), (105) and (112) [35,36], also, peaks at approximately 38.3° and 64.6° suggested the presence of the

AuNPs (111) and (220) [37] (JCPDS 04-0784). These observations confirmed the successful preparation of the MoS_2-AuNPs nanoparticles (b, Fig. 1H).

3.2. Electrochemical properties of the Chox/MoS_2–AuNPs/GCE

The electrochemical properties of the Chox/MoS_2-AuNPs/GCE were investigated with the use of the electrochemical impedance spectroscopy (EIS), cyclic voltammetry (CV) and chronocoulometry (Fig. 2). The experiments were performed in 5×10^{-3} mol L^{-1} $[Fe(CN)_6]^{3-/4-}$ (1:1) solution containing 0.1 mol L^{-1} KCl.

The Z' (real part) versus Z'' (imaginary part) of the EIS graph indicated that the electron-transfer resistance (Ret) at the electrode surface was the same as the diameter of the semicircle on the Nyquist plot and can be used to describe the properties at the interface of the electrode [38]. The profile, which displayed a small well-defined semi-circle (Ret) at higher frequencies, was obtained from the untreated GCE (curve a, Fig. 2A). This indicated a small impedance at the interface. Also, when MoS_2 was covered on the surface of the GCE, the impedance curve of the modified electrode consisted of a large semicircle, and the electron transfer resistance was high, as well. This indicated that the MoS_2/GCE (b, Fig. 2A) has poor conductivity, attributed to the cross-linking agent (Nafion film) itself introducing resistance into the electrode/solution system [39]. However, when the AuNPs were deposited on the MoS_2/GCE surface, the Ret of MoS_2-AuNPs/GCE decreased obviously (c, Fig. 2A). This result indicated that the MoS_2-AuNPs had good conductivity. Finally, the Chox/MoS_2-AuNPs/GCE (d, Fig. 2A) was tested and a larger semicircle was noted compared to that in the above cases. This observation indicated that Chox was immobilized on the MoS_2-AuNPs/GCE as a film.

CV experiments with the electrode systems as above and in the presence of same redox probe, $[Fe(CN)_6]^{3-/4-}$, produced the results as in Fig. 2B, which reflected the conclusions obtained from the EIS work above. Due to the redox probe of $[Fe(CN)_6]^{3-/4-}$, the untreated GCE showed a pair of well defined redox peak (curve a, Fig. 2B). When MoS_2 were modified on the GCE, the redox peak current decreased (b, Fig. 2B) since the cross-linking agent (Nafion film) with negative charge can hinder the electron transference. After that, when AuNPs were deposited on the MoS_2/GCE surface, the redox peak current obviously increased due to the good conductivity of AuNPs (c, Fig. 2B). Finally, the Chox/MoS_2-AuNPs/GCE was tested (d, Fig. 2B), and the redox peak current of $[Fe(CN)_6]^{3-/4-}$ was effectively absent since Chox disturb the electron transfer.

Chronocoulometric results from the reduction of $[Fe(CN)_6]^{3-/4-}$ (5×10^{-3} mol L^{-1}) with KCl (0.1 mol L^{-1}) obtained from different electrodes were used to compare the apparent electrode areas with the use of Eq. (1) [40]:

$$Q(t) = (2nFAD_0{}^{1/2}\pi^{-1/2}c_0)t^{1/2} \quad (1)$$

where $Q(t)$ – absolute value of the reduction charge, n – number of electrons transferred, F – Faraday constant, A – the apparent electrode area, t – time, and D_0 and c_0 – diffusion coefficient and the bulk concentration of the oxidized form of the hexacyanoferrate (III) complex, respectively. Here A can be estimated from the slope of the $Q(t)$ versus $t^{1/2}$ plot (Fig. 2C). Thus, the order of the slope values was: MoS_2-AuNPs/GCE(c) > MoS_2/GCE(b) > GCE(a), i.e. MoS_2-AuNPs/GCE has the largest A value.

3.3. Electro-catalysis of cholesterol at the differently modified electrodes

Fig. 3A shows the CVs of the Chox/MoS_2-AuNPs/GCE in 0.05 M PBS (pH 7.0) without (curve a) and with (curve b) 10.0 μM cholesterol. It clearly showed that the oxidation current increased greatly

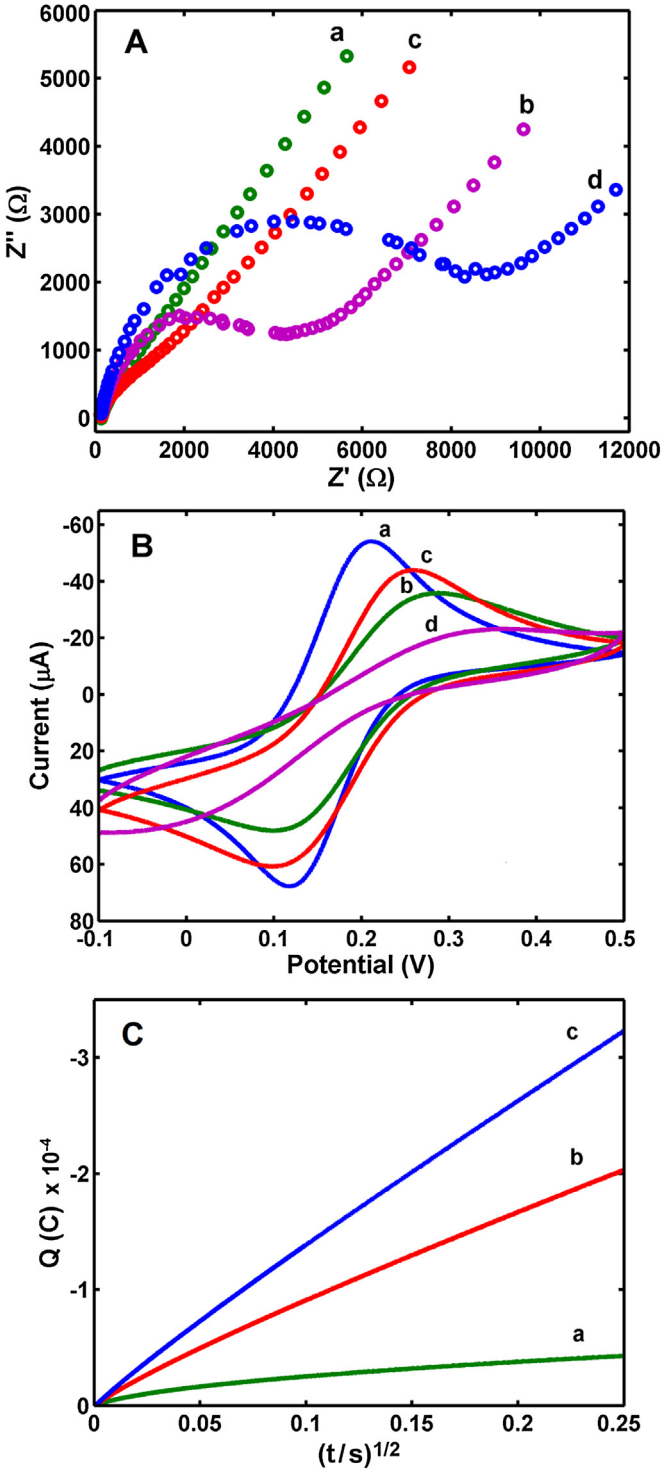

Fig. 2. (**A**) Electrochemical impedance spectroscopy (EIS) and (**B**) cyclic voltammograms of: (**a**) GCE, (**b**) MoS_2/GCE, (**c**) MoS_2-AuNPs/GCE, and (**d**) Chox/MoS_2-AuNPs/GCE in 5×10^{-3} mol L^{-1} $[Fe(CN)_6]^{3-/4-}$ (1:1) solution containing 0.1 M KCl; (**C**) chronocoulometric curves of (**a**) GCE, (**b**) MoS_2/GCE, and (**c**) MoS_2-AuNPs/GCE for the reduction of 5×10^{-3} mol L^{-1} $K_3[Fe(CN)_6]$ in 0.1 mol L^{-1} KCl.

after the addition of cholesterol. This indicated that the modified electrode had excellent catalytic performance toward cholesterol.

The pH 7.0 and operational potential of +0.30 V (see Fig. S1, Supplementary material) were chosen for subsequent amperometric measurements for cholesterol. To investigate the performance of the differently modified electrodes, the current-time amperometric curves of the electrodes were recorded under the conditions

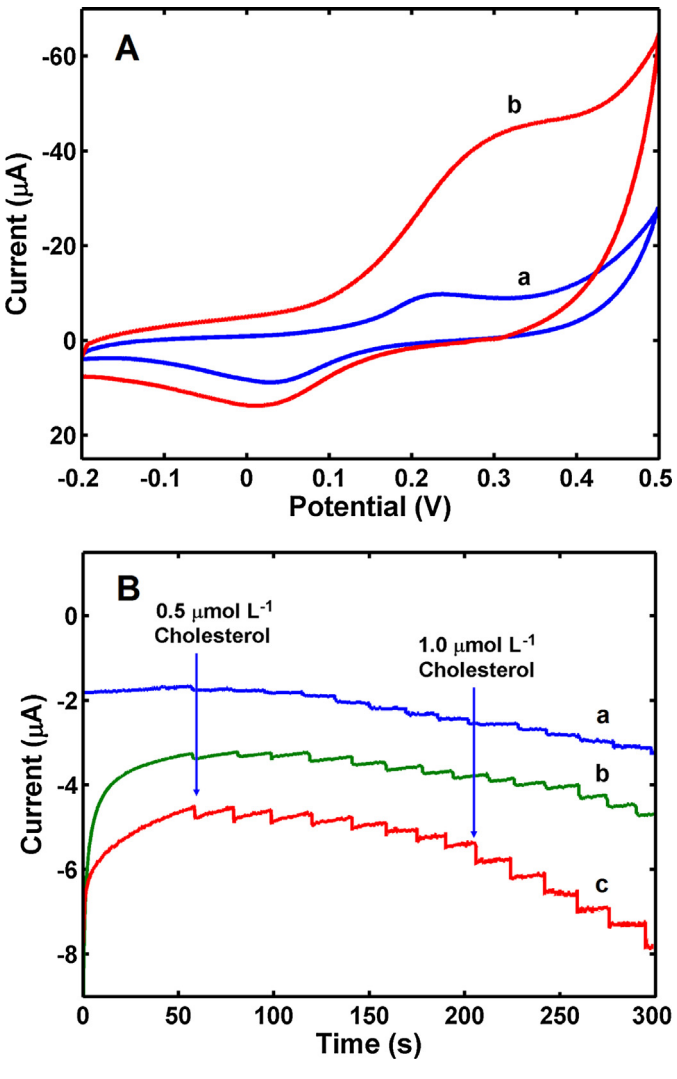

Fig. 3. (**A**) CVs of the Chox/MoS_2-AuNPs/GCE in the (**a**) absence and (**b**) presence of 10.0 μM cholesterol in 0.05 M PBS (pH 7.0) at 0.10 V s^{-1}. (**B**) Amperometric response recorded at (**a**) Chox/MoS_2/GCE, (**b**) Chox/AuNPs/GCE and (**c**) Chox/MoS_2-AuNPs/GCE.

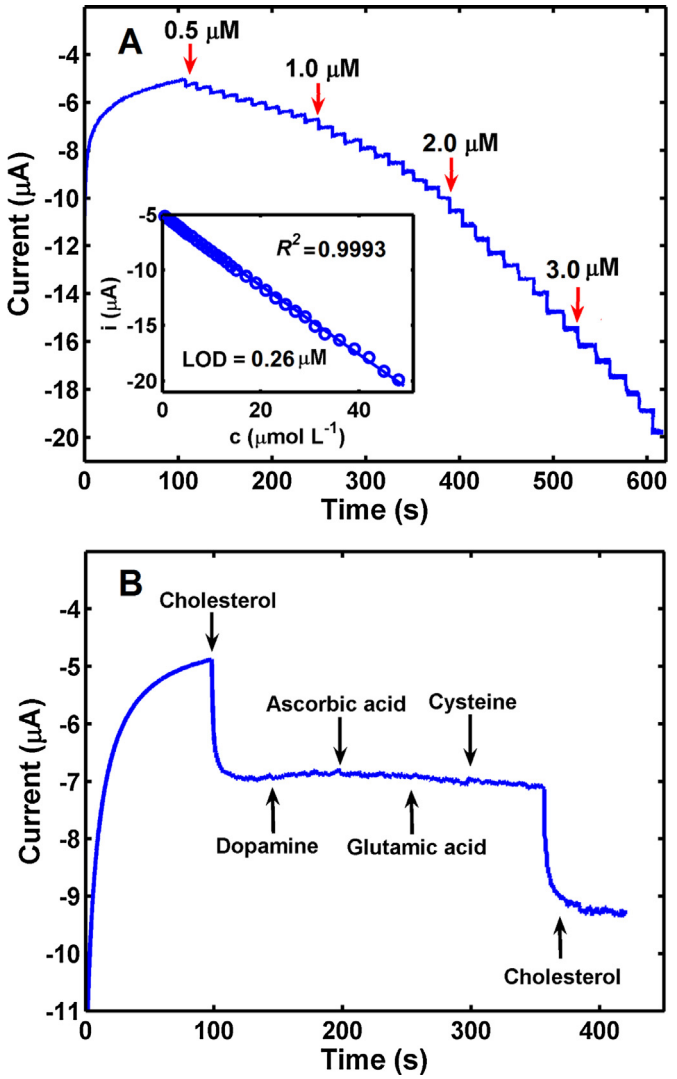

Fig. 4. (**A**) Amperometric response of the Chox/MoS_2-AuNPs/GCE obtained under the conditions of continuous stirring and successive step changes of cholesterol at +0.30 V in 0.05 M PBS (pH 7.0). Inset: Calibration plot of the Chox/MoS_2-AuNPs/GCE presented as a function of cholesterol concentration. (**B**) An interference study with the use of successive additions of 5 μM cholesterol to each of the following substances: 1.0 mM dopamine, 1.0 mM ascorbic acid, 1.0 mM glutamic acid and 1.0 mM cysteine and 5 μM cholesterol. Each sample was analysed separately under the conditions of continuous stirring of the solution at +0.30 V in 0.05 M PBS (pH 7.0).

of continuous stirring of the solution and successive step changes of cholesterol at +0.30 V in PBS (pH 7.0) (as shown in Fig. 3B). The results indicated that Chox/MoS_2/GCE did catalyse cholesterol (curve a, Fig. 3B), but a much stronger catalytic current was observed for Chox/AuNPs/GCE (b, Fig. 3B). When AuNPs and MoS_2 were combined, the catalytic current of cholesterol was obviously increased (c, Fig. 3B). This improvement can be attributed to the synergistic catalytic effect of AuNPs and MoS_2. Also, this observation can be explained by noting that the MoS_2-AuNPs/GCE has a larger surface area, and thus, is able to adsorb more Chox molecules. From these results it was evident that the GCE, on which an MoS_2-AuNPs coating was deposited, was actually an effective sensing platform for the immobilization of Chox.

3.4. Quantitative analysis of cholesterol

Quantitative analysis of cholesterol was performed with the use of the amperometric $i-t$ technique under the conditions of continuous stirring of the solution and successive step changes of cholesterol at +0.30 V in PBS (pH 7.0). The response current versus concentration plot for cholesterol was linear in range of 0.5–48 μM (Fig. 4A), and the corresponding limit of detection (LOD) was 0.26 ± 0.015 μM. Furthermore, the sensitivity of the sensor was calculated to be 4460 μA mM^{-1} cm^{-2}. The performance of the novel method for the analysis of cholesterol described in this work, is evidently quite competitive with other available methods when the comparison is based on the electrode materials, analytical range, sensitivity and LOD values (see Table S1, Supplementary material).

The apparent Michaelis-Menten constant (K_M^{app}), which gives an indication of the enzyme-substrate kinetics for the biosensors, can be calculated from the electrochemical version of the Lineweaver-Burk equation [41,42].

$$\frac{1}{I} = \frac{1}{I_{max}} + \frac{K_M^{app}}{I_{max}C} \quad (2)$$

where c is the concentration of cholesterol in solution, I is the catalytic reduction current (background current deducted) at the steady state when cholesterol concentration is c, and I_{max} is the maximum catalytic current. The K_M^{app} value for the cholesterol senor was determined by the analysis of the slope and intercept for the plot of the reciprocals of steady-state current versus cholesterol

Table 1
Determination of cholesterol in egg yolk and pork liver samples by the proposed method ($n = 3$).

Samples	Content (mg g^{-1})	Spiked (mg g^{-1})	Found (mg g^{-1})	%Recovery
#1[a]	3.78	2.00	5.63 (±0.14)	96.0[b]
#2	3.96	2.00	5.86 (±0.21)	97.5
#3	18.63	10.00	28.98 (±0.28)	101.9
#4	21.26	10.00	30.77 (±0.31)	97.7

[a] Samples #1 and #2: **pork liver**; #3 and #4: **egg yolk**–purchased from a super market in Nanchang city.
[b] %Recovery = $100 \times (c_{\text{Found}} - c_{\text{spiked}})/c$.

concentrations, i.e. the Lineweaver-Burk plot of $1/I$ vs. $1/c$ (Fig. S2, Supplementary material). According to the Lineweaver-Burk plot, the K_M^{app} is calculated to be 0.325 mM. As well known, the smaller of K_M^{app}, the higher catalytic ability of the cholesterol biosensor possesses.

3.5. Interferences, reproducibility and stability

Selectivity of the novel method was investigated at the Chox/MoS_2-AuNPs/GCE under the same conditions, and different common interfering substances were used, e.g. dopamine, ascorbic acid, glutamic and cysteine. The current versus potential plot (Fig. 4B) clearly indicated that these compounds produced little interference during the analysis of cholesterol, i.e. the electrode fabricated for this work was selective for sensing cholesterol in the presence of interfering compounds noted above.

A cholesterol sample (10.0 μM) was used for quantitative analysis to evaluate the reproducibility and stability of the modified electrode, Chox/MoS_2-AuNPs/GCE. The procedure was repeated four more times for the same cholesterol sample, and total five results were collected. The average relative standard deviation (%RSD) of was 4.87%, and it indicated the satisfactory and acceptable reproducibility for the modified biosensor.

The stability of the biosensor was further assessed by storing it at 4 °C for 15 days, and the biosensor returned a reading of 92.1% of the original response on the cholesterol sample of 10.0 μM. This result suggested that the cholesterol biosensor is quite stable for the analysis of the analyte over at least 14 days. Also, the stability of the modified electrode may be attributed to the presence of MoS_2-AuNPs nano-particles, which provided a microenvironment that facilitates the bioactivity of Chox. In addition, it is possible that 0.05% Nafion could contribute to the protection of Chox.

3.6. Analytical application: cholesterol in raw egg yolk and pork samples

To demonstrate some practical applications of the novel method, the fabricated electrode was used for the determination of cholesterol in raw egg yolk and pork samples. A suitable amount of PBS (pH 7.0) was transferred in an electrolysis cell, and was subjected to amperometric i–t scan at a constant potential of +0.3 V until a steady current was obtained. Then, separately, a processed sample (100 μL) of pretreated egg yolk or pork liver (see Section 2.5) was added to the electrolysis cell, and an amperometric i–t profile was recorded. Furthermore, standard addition method was carried out to test the recovery of the proposed method. A suitable amount of PBS (pH 7.0) was transferred to the cell, then, an analyte sample (100 μL egg yolk or 100 μL pork liver) together with an appropriate cholesterol standard solution were added to the cell, and the i–t profile was recorded as above. The obtained results (Table 1) indicated that the analyses for cholesterol in egg and pork samples were acceptable and reliable.

4. Conclusions

A sensitive biosensor, Chox/MoS_2-AuNPs/GCE, has been successfully constructed to analyse the cholesterol with the use of a step by step method. The good sensitivity and stability were attributed to the synergistic catalytic effects of the MoS_2 and AuNPs. In addition, the relatively large surface area of the MoS_2-AuNPs/GCE and its ability to absorb readily the Chox molecules were favorable for the successful analysis. To demonstrate the practical application, this biosensor was used for the quantitative analyses of cholesterol in egg yolk and pork liver samples with successful recoveries (96.0–101.9%). Importantly, these results also showed that the MoS_2-AuNPs was an effective sensing platform for the immobilization of Chox.

Acknowledgements

The authors gratefully acknowledge the financial support of this study by the National Natural Science Foundation of China (NSFC−31401587), the Natural Science Foundation of Jiangxi Province, China (20142BAB213009), and the State Key Laboratory of Food Science and Technology of Nanchang University (SKLF−ZZA-201612).

Appendix A. Supplementary data

Supplementary data associated with this article can be found, in the online version, at http://dx.doi.org/10.1016/j.snb.2016.04.019.

References

[1] H.F. Zhang, R.X. Liu, J.B. Zheng, Selective determination of cholesterol based on cholesterol oxidase- alkaline phosphatase bienzyme electrode, Analyst 137 (2012) 5363–5367.
[2] M.H. Zhang, R. Yuan, Y.Q. Chai, C. Wang, X.P. Wu, Cerium oxide–graphene as the matrix for cholesterol sensor, Anal. Biochem. 436 (2013) 69–74.
[3] C.Y. Wang, X.R. Tan, S.H. Chen, R. Yuan, F.X. Hu, D.H. Yuan, Highly-sensitive cholesterol biosensor based on platinum–gold hybrid functionalized ZnO nanorods, Talanta 94 (2012) 263–270.
[4] R.M. Li, C. Xiong, Z.Y. Xiao, L.S. Ling, Colorimetric detection of cholesterol with G-quadruplex-based DNAzymes and ABTS(2-), Anal. Chim. Acta 724 (2012) 80–85.
[5] J.H. Li, Z. Zhang, S.F. Xu, L.X. Chen, N. Zhou, H. Xiong, H.L. Peng, Label-free colorimetric detection of trace cholesterol based on molecularly imprinted photonic hydrogels, J. Mater. Chem. 21 (2011) 19267–19274.
[6] T. Larsen, Enzymatic-fluorometric quantification of cholesterol in bovine milk, Food Chem. 135 (2012) 1261–1267.
[7] J. Galban, J.F. Sierra, J.M.L. Sebastian, S. De Marcos, J.R. Castillo, Direct fluorometric determination of total cholesterol in serum using derivatized cholesterol oxidase, Appl. Spectrosc. 54 (2000) 1157–1162.
[8] D.M. Amundson, M.J. Zhou, Fluorometric method for the enzymatic determination of cholesterol, J. Biochem. Bioph. Methods 38 (1999) 43–52.
[9] D.N. Clausen, J.V. Visentainer, C.R.T. Tarley, Development of molecularly imprinted poly(methacrylic acid)/silica for clean-up and selective extraction of cholesterol in milk prior to analysis by HPLC-uV, Analyst 139 (2014) 5021–5027.
[10] A. Kotani, H. Hakamata, N. Nakayama, F. Kusu, Picomole level determination of cholesterol by HPLC with electrochemical detection using boron-doped diamond electrode after performance assessment based on the FUMI theory, Electroanalysis 23 (2011) 2709–2715.
[11] K.M. Phillips, D.M. Ruggio, J.A. Bailey, Precise quantitative determination of phytosterols, stanols, and cholesterol metabolites in human serum by capillary gas-liquid chromatography, J. Chromatogr. B 732 (1999) 17–29.
[12] V. Cardenia, M.T. Rodriguez-Estrada, M.T. Rodriguez-Estrada, E. Baldacci, S. Savioli, G. Lercker, Analysis of cholesterol oxidation products by fast gas chromatography-mass spectrometry, J. Sep. Sci. 3 (2012) 424–430.
[13] M.M. Rahman, A.M. Asiri, One-step electrochemical detection of cholesterol in the presence of suit $K_3Fe(CN)_6$/phosphate buffer mediator by an electrochemical approach, Talanta 140 (2015) 96–101.
[14] M. Srivastava, S.K. Srivastava, N.R. Nirala, R. Prakash, A chitosan-based polyaniline-au nanocomposite biosensor for determination of cholesterol, Anal. Methods 6 (2014) 817–824.
[15] X. Ou, X.R. Tan, S.P. Wei, S.H. Chen, J.J. Zhang, X.F. Liu, Electrochemiluminescence biosensor for cholesterol detection based on AuNPs/L-cys–C60 nanocomposites, Anal. Methods 6 (2014) 3804–3810.

[16] A.K. Giri, C. Charan, A. Saha, V.K. Shahi, A.B. Panda, An amperometric cholesterol biosensor with excellent sensitivity and limit of detection based on an enzyme-immobilized microtubular ZnO@ZnS heterostructure, J. Mater. Chem. A 2 (2014) 16997–17004.
[17] L. Xu, M.D. Zhang, Y.T. Hou, W. Huang, C. Yao, Q. Wu, An Au nanocomposite based biosensor for determination of cholesterol, Anal. Methods 7 (2015) 3480–3485.
[18] R. Ahmad, N. Tripathy, J.H. Park, Y.B. Hahn, A comprehensive biosensor integrated with a ZnO nanorod FET array for selective detection of glucose, cholesterol and urea, Chem. Commun. 51 (2015) 11968–11971.
[19] H. Dhyani, M.A. Ali, S.P. Pal, S. Srivastava, P.R. Solanki, B.D. Malhotra, P. Sen, Mediator-free biosensor using chitosan capped CdS quantum dots for detection of total cholesterol, RSC Adv. 5 (2015) 45928–45934.
[20] X. Ou, X.R. Tan, X.F. Liu, H.M. Chen, Y. Fan, S.H. Chen, S.P. Wei, A cathodic luminol-based electrochemiluminescence biosensor for detecting cholesterol using 3D-moS_2–PANI nanoflowers and Ag nanocubes for signal enhancement, RSC Adv. 5 (2015) 66409–66415.
[21] M.M. Rahman, reusable and mediator-free cholesterol biosensor based on cholesterol oxidase immobilized onto TGA-sAM modified smart nio-chips, PLoS One 9 (2014) e100327.
[22] B. Bajaj, H.I. Joh, S.M. Jo, G. Kaur, A. Sharma, M. Tomar, V. Gupta, S. Lee, Controllable one step copper coating on carbon nanofibers for flexible cholesterol biosensor substrates, J. Mater. Chem. B 2 (2016) 229–236.
[23] B. Gao, H.Q. Fan, X.J. Zhang, Hydrothermal synthesis of single crystal MoO_3 nanobelts and their electrochemical properties as cathode electrode materials for rechargeable lithium batteries, J. Phys. Chem. Solids 73 (2012) 423–429.
[24] B. Gao, H.Q. Fan, X.J. Zhang, C.J. Zhu, Template-free hydrothermal synthesis of α-molybdenum trioxide nanobelts and their photocatalytic activity for degradation of methylene blue, Micro Nano Lett. 8 (2013) 500–503.
[25] Z. Peng, L. Jing, W. Lin, B.H. Zhao, L.X. Yang, H.Q. Fan, Preparation and characterization of molybdenum particles by reducing MoO_3 nano-fibers, Synth. React. Inorg. M 38 (2008) 318–321.
[26] Y. Feldman, E. Wasserman, D.J. Srolovitz, R. Tenne, High-rate, gas-phase growth of MoS_2 nested inorganic fullerenes and nanotubes, Science 267 (1995) 222–225.
[27] T.Y. Wang, H.C. Zhu, J.Q. Zhuo, Z.W. Zhu, P. Papakonstantinou, G. Lubarsky, J. Lin, M. Li, Biosensor based on ultrasmall MoS_2 nanoparticles for electrochemical detection of H_2O_2 released by cells at the nanomolar level, Anal. Chem. 85 (2013) 10289–10295.
[28] B. Radisavljevic, A. Radenovic, J. Brivio, V. Giacometti, A. Kis, Single-layer MoS_2 transistors, Nature Nanotechnol. 6 (2011) 147–150.
[29] D.J. Late, B. Liu, H.S.S.R. Matte, V.P. Dravid, C.N.R. Rao, Hysteresis in single-layer MoS_2 field effect transistors, ACS Nano 6 (2012) 5635–5641.
[30] T.Y. Wang, K.Z. Du, W.L. Liu, J.X. Zhang, M.X. Li, Electrochemical sensors based on molybdenum disulfide nanomaterials, Electroanalysis 27 (2015) 2091–2097.
[31] Q.H. Wang, K. Kalantar-Zadeh, A. Kis, J.N. Coleman, M.S. Strano, Electronics and optoelectronics of two-dimensional transition metal dichalcogenides, Nature Nanotechnol. 7 (2012) 699–712.
[32] T.S. Sreeprasad, P. Nguyen, N. Kim, V. Berry, Controlled, defect-guided, metal-nanoparticle incorporation onto MoS_2 via chemical and microwave routes: electrical, thermal, and structural properties, Nano Lett. 13 (2013) 4434–4441.
[33] X. Wang, C.C. Chu, L. Shen, W.P. Deng, M. Yan, S.G. Ge, J.H. Yu, X.R. Song, An ultra sensitive electrochemical immunosenso rbased on the catalytical activity of MoS_2-Au composite using Ag nanospheresas labels, Sensor. Actuat. B – Chem. 206 (2015) 30–36.
[34] X.Y. Lin, Y.N. Ni, S. Kokot, Glassy carbon electrodes modified with gold nanoparticles for the simultaneous determination of three food antioxidants, Anal. Chim. Acta 765 (2013) 54–62.
[35] X.R. Guo, Y. Wang, F.Y. Wu, Y.N. Ni, S. Kokot, A colorimetric method of analysis for trace amounts of hydrogen peroxide with the use of the nano-properties of molybdenum disulfide, Analyst 140 (2015) 1119–1126.
[36] D.Z. Wang, Z.P. Wang, C.L. Wang, P. Zhou, Z.Z. Wu, Z.H. Liu, Distorted MoS_2 nanostructures: an efficient catalyst for the electrochemical hydrogen evolution reaction, Electrochem. Commun. 34 (2013) 219–222.
[37] L. Shang, F.Q. Zhao, B.Z. Zeng, Electrocatalytic oxidation and determination of hydrazine at an AuCu nanoparticles-graphene-ionic liquid composite film coated glassy carbon electrode, Electroanalysis 24 (2012) 2380–2386.
[38] X.Y. Lin, Y.N. Ni, S. Kokot, An electrochemical DNA-sensor developed with the use of methylene blue as a redox indicator for the detection of DNA damage induced by endocrine-disrupting compounds, Anal. Chim. Acta 867 (2015) 29–37.
[39] H.S. Yin, Y.L. Zhou, Q. Ma, S.Y. Ai, P. Ju, L.S. Zhu, L.A. Lu, Electrochemical oxidation behavior of guanine and adenine on graphene-nafion composite film modified glassy carbon electrode and the simultaneous determination, Process Biochem. 45 (2010) 1707–1712.
[40] X.Y. Lin, Y.N. Ni, S. Kokot, Electrochemical and bio-sensing platform based on a novel 3D Cu nano-flowers/layered MoS_2 composite, Biosens. Bioelectron. 79 (2016) 685–692.
[41] A. Umar, M.M. Rahman, A. Al-Hajry, Y.B. Hahn, Highly-sensitive cholesterol biosensor based on well- crystallized flower-shaped ZnO nanostructures, Talanta 78 (2009) 284–289.
[42] X.H. Liu, Z.H. Nan, Y. Qiu, L.C. Zheng, X.Q. Lu, Hydrophobic ionic liquid immoblizing cholesterol oxidase on the electrodeposited Prussian blue on glassy carbon electrode for detection of cholesterol, Electrochim. Acta 90 (2013) 203–209.

Biographies

Xiaoyun Lin received his BS degree from Gannan Normal University, China, in 2002. Then, he received his MS and PhD degrees from Nanchang University, China, in 2005 and 2013, respectively. He is currently an associate professor in College of Chemistry, Nanchang University, China. His current research interests include electrochemical sensor and synthesis of nano-materials.

Yongnian Ni received his BS and MS degrees from East China University of Science and Technology, Shanghai, China, in 1970 and 1982, respectively. He is now a Professor in College of Chemistry, Nanchang University, China. His current research interests include electroanalysis, sensors and applied chemometrics.

Serge Kokot (BSc (Hons) PhD (1965–1972), UNSW, Australia). At present, he is an Associate Professor (adj.), School of Chemistry, Physics and Mechanical Engineering, QUT, Brisbane, Australia, a Fellow of the Royal Australian Chemical Institute (FRACI) and a recipient of the RACI Analytical Chemistry Division medal, 2006 (the inaugural Prof. Lloyd Smyth). He is a co-author of about 250 chemistry related publications and his current research interests include analytical and environmental chemistry as well as applied chemometrics.